Localization of Abnormal EEG Sources Using Blind Source Separation Partially Constrained by the Locations of Known Sources

Mohamed Amin Latif, *Member, IEEE*, Saeid Sanei, *Senior Member, IEEE*, Jonathon Chambers, *Senior Member, IEEE*, and Leor Shoker, *Member, IEEE*

***Abstract*—Electroencephalogram (EEG) source localization requires a solution to an ill-posed inverse problem. The additional challenge is to solve this problem in the context of multiple moving sources. An effective and simple technique for both separation and localization of EEG sources is therefore proposed by incorporating an algorithmically coupled blind source separation (BSS) approach. The method relies upon having *a priori* knowledge of the locations of a subset of the sources. The cost function of the BSS algorithm is constrained by this information, and the unknown sources are iteratively calculated. An important application of this method is to localize abnormal sources, which, for example, cause changes in attention, movement, and behavior. In this application, the Alpha rhythm was considered as the known sources. Simulation studies are presented to support the potential of the approach in terms of source localization.**

***Index Terms*—Blind source separation (BSS), electroencephalogram (EEG), partially constrained, source localization.**

I. Introduction

ELECTROENCEPHALOGRAM (EEG) signals can be used as one of the sources of information for the diagnosis of anatomical, functional pathological, and physiological abnormalities in the brain. These signals include normal and abnormal rhythms within the frequency range of 0.3 to more than 40 Hz. This range is divided into five main subbands of 0.3–3.5 Hz (Delta), 3.5–7.5 Hz (Theta), 7.5–13 Hz (Alpha), 13–30 Hz (Beta), and more than 30 Hz (Gamma). Localization of abnormal sources within the brain has been an important problem within both the neurophysiology and signal processing communities. A number of methods for localization of EEG sources have been investigated by researchers. These methods can be divided into two main categories: "equivalent current dipole" approach, in which the EEG signals are assumed to be generated by a relatively small number of focal sources, and the "linear distributed" approach, in which all possible source locations are considered simultaneously [21]. Among the current dipole approaches, the methods based on a dipole assumption for the sources have been very well established. The dipole methods such as MUSIC [1] and RAP-MUSIC [5] have been extended to estimation of the source locations. Also, there have been some algorithms based on the linear distributed approach, some of which have already commercialized [14], such as minimum $\ell_P(\ell_1, \ell_{1.5}, \ell_2)$ norm and low-resolution tomography (LRT) or LORETA [12], [13]. However, the accuracy of such algorithms is dependent on the number of both sources and sensors, assuming fixed positions of the sources [2]. Moreover, in most of the above algorithms, a head volume conductor model and a source model have to be defined. Therefore, the associated computational complexity is generally very high. Other techniques solely based on independent component analysis (ICA) cannot ensure a unique solution to the problem [7]. In most of the localization research [2], [4], [6], [8] for solving the forward problem, the accuracy of the solution is highly dependent on the assumption about the number and location of the sources. It also requires the parameters and geometry of the head model. Commonly, only the head surface and cortical surface positions of the sources are considered [3]. Therefore, this approach is still an open problem. The experimental and clinical problem, however, is the inverse problem of finding the distribution of currents inside the head, based on electric and magnetic recordings outside the head. This is fundamentally an ill-posed problem since it has no unique solution. For any set of measurements outside the head, there are infinitely many current distributions inside the head that are compatible with those recordings. In this letter, we develop a new ICA-based linear distributed approach to attempt to obtain a unique solution to the localization problem. In this method, it is assumed that the EEG sources are independent. The independence assumption for certain brain signals is perhaps weak, but this assumption has been found to be strong for the abnormal or event-related sources. In addition, the locations of the normal brain rhythms for healthy adults, without any attention, visual, or possibly auditory stimulation, and without dysfunction of the central nerve system (CNS), are considered to be known (obtained from the EEG recordings carefully filtered within specific bands) [15]. The power of the bandpass normal rhythm is an estimate of the neural power originating from the normal source, which generates a clue for the location of the known sources. We can also consider other normal brain rhythms, with their known locations, as potential constrains. This can be achieved automatically by detecting the peaks of signals within each conventional band. However, the actual locations are dependent on many factors, such as physical condition and age of the subject. The instantaneous BSS formulation is as follows. Denote the observed signals by $\mathbf{x} = [x_1(t), x_2(t), \ldots, x_n(t)]^T$, where $\mathbf{x} \in \mathbb{R}^n$ and the unknown independent sources by

Manuscript received July 2, 2005; revised October 3, 2005. The associate editor coordinating the review of this manuscript and approving it for publication was Dr. Dimitri Van De Ville.

The authors are with the Centre of Digital Signal Processing, Cardiff School of Engineering, Cardiff University, Cardiff CF24 3AA, U.K. (e-mail: latifa@cf.ac.uk; saneis@cf.ac.uk; chambersj@cf.ac.uk; shokerl@cf.ac.uk).

Digital Object Identifier 10.1109/LSP.2005.862622

$\mathbf{s} = [s_1(t), s_2(t), \ldots, s_m(t)]^T$, where $\mathbf{s} \in \mathbb{R}^m$, and t denotes descrete time

$$\mathbf{x} = \mathbf{A}\mathbf{s} + \mathbf{v} \tag{1}$$

and

$$\mathbf{y} = \mathbf{W}\mathbf{x} \tag{2}$$

where $\mathbf{v} \in \mathbb{R}^n$ is assumed to be a white zero-mean Gaussian noise vector, $\mathbf{A} \in \mathbb{R}^{n\times m}$ and $\mathbf{W} \in \mathbb{R}^{m\times n}$ are unknown constant mixing and unmixing matrices, respectively (in convolutive case $\mathbf{x} = \mathbf{A} * \mathbf{s} + \mathbf{v}$, and $\mathbf{y} = \mathbf{W} * \mathbf{x}$, where $*$ represents the convolution operation), and $(.)^T$ is vector transpose. The mixture is assumed to be over-determined (valid for usual cases), i.e., $m < n$, and $\mathbf{y} = [y_1(t), y_2(t), \ldots, y_m(t)]^T$, where $\mathbf{y} \in \mathbb{R}^m$ is the output of the blind source separation (BSS) system, which is an estimate of the sources $\mathbf{s}$. The separation matrix W can be found by finding the global minima (or maxima) of a cost function $J_m(W)$, which provides a measure of independency of the estimated sources. Using ICA, we can attempt to separate the signals into their independent components. The number of outputs may be approximated by one of the methods described in [6]. However, the separation is subject to the scaling and permutation of the sources, i.e.,

$$\mathbf{A} = \mathbf{D}\mathbf{R}\mathbf{W}^{-1} \tag{3}$$

where $\mathbf{D}$ and $\mathbf{R}$ are the scaling and permutation matrices, respectively, and $\mathbf{W}^{-1}$ is the pseudo inverse. The effect of $\mathbf{D}$ can be constrained by the size of the head, and it can be generally disabled by normalization of the estimated separating matrix after each iteration. However, without solving the permutation problem, no solution to the estimation of $\mathbf{A}$ will be possible. This means there will be no clue to finding a unique solution to the localization problem. However, *a priori* information about the locations of some of the sources, say, $k < m$, can lead to a more accurate estimation of $\mathbf{A}$ and, as a result, the locations of other sources. The known sources can be either the normal brain rhythms for a fully alert and awake person, such as the Alpha rhythm, which can be filtered and used, or a number of synthetic sources located around the brain through the mouth or nose.

II. Source Localization

Assuming the head as a homogenous medium, the link weights are inversely proportional to the attenuation of the signals crossing the brain tissues, i.e., $a_{ij} \approx \Gamma_{ij}^{-1}$. To formulate the problem, consider k out of m sources are known. This means that the scaled values of the k columns of $\mathbf{A}$ are known. We define a new matrix as $\tilde{\mathbf{A}}$ such that its columns correspond to the known and the unknown sources the element of which are represented by a_{ij}^{k} and a_{ij}^{uk}, respectively. In this case

$$\tilde{\mathbf{A}} = [A_k \vdots A_{uk}] = \begin{bmatrix} a_{11}^k \ldots a_{1k}^k & a_{1k+1}^{uk} \ldots a_{1m}^{uk} \\ \vdots & \vdots \\ a_{n1}^k \ldots a_{nk}^k & a_{nk+1}^{uk} \ldots a_{nm}^{uk} \end{bmatrix} \tag{4}$$

where A_k, $n \times k$, and A_{uk} $n \times (m-k)$ are, respectively, the known and unknown submatrices. In most of the BSS algorithms, $\mathbf{W}$ is calculated iteratively in order to obtain the most statistically independent sources. Now, during the separation process, we may simultaneously try to enforce the following constraint:

$$\mathbf{J}_c = \|\tilde{\mathbf{A}} - \mathbf{R}\mathbf{W}^{-1}\|_F^2 = trace\left([\tilde{\mathbf{A}} - \mathbf{R}\mathbf{W}^{-1}][\tilde{\mathbf{A}} - \mathbf{R}\mathbf{W}^{-1}]^T\right) \tag{5}$$

where $\|.\|_F^2$ is the Frobenius norm. In this equation, $\mathbf{D}$ is discarded since $\mathbf{W}$ is normalized after each iteration. This constraint is then incorporated into the main BSS cost function, resulting in an unconstrained problem for finding $\mathbf{W}$. At the same time, $\mathbf{R}$ and A_{uk} are estimated iteratively based on an algorithmically coupled method, as described in Section III. In order to locate the sources more accurately, the nonhomogeneity of the head region has to be exploited. A novel method is described in Section IV to solve this problem.

III. Constrained Problem

EEG signals are statistically nonstationary. They are affected by other human internal signals, such as heart beat, noise of the measurement system, environment noise, and interference from the adjacent electrode signals. In this letter, we assume that the effects of system noise and other human internal signals are filtered out. The effective bandwidth for EEGs is from 0.3 to 40 Hz. Since each electrode signal is in fact a combination of more than one nearby source, blind separation of these signals appears to be favorable, whereby additional information beyond correlation functions is exploited. Since the signals are not stationary, an accurate separation technique may be, however, hard to achieve. A number of recently developed techniques such as time-lagged second-order blind identification (SOBI) [20] or as [9] can better cope with nonstationarity of the data. On the other hand, the signals may be considered stationary within short segments of about 10 s (or about 2000 samples). Since our main objective is localization of the sources having *a priori* information about locations of some of the sources, the particular separation method is of less concern. A natural and common criterion for joint approximation diagonalization (JAD) is the least-squares (LS) approach [10]. Therefore, to find $\mathbf{W}$ and $\mathbf{R}$, we can add a constraint to the LS cost function and solve the following unconstrained problem:

$$\mathbf{J}(\mathbf{W}) = \mathbf{J}_m(\mathbf{W}) + \lambda \mathbf{J}_c(\mathbf{W}) \tag{6}$$

where $\mathbf{J}_m(\mathbf{W})$ is the main LS BSS cost function, $\mathbf{J}_c(\mathbf{W})$ is the constraint defined by (5), and λ is the Lagrange multiplier. To minimize (6), the following update is used:

$$\mathbf{W}_{t+1} = \mathbf{W}_t - \mu \nabla_{\mathbf{W}} \mathbf{J} \tag{7}$$

where $\mathbf{J}$ is defined in (6), μ is the learning rate, and ∇ denotes the gradient operator. Therefore, we have

$$\nabla_{\mathbf{W}} \mathbf{J}_c = 2\left(\mathbf{W}_t^{-1}\tilde{\mathbf{A}}_t^T \mathbf{R}_t \mathbf{W}_t^{-1}\right)^T - \mathbf{W}_t\left(\mathbf{W}_t^T\mathbf{W}_t\right)^{-1}\left(\mathbf{R}_t^T\mathbf{R}_t\right)\left(\mathbf{W}_t^T\mathbf{W}_t\right)^{-1} \tag{8}$$

(when $m \neq n$, $\mathbf{W}^{-1}$ will be the pseudo inverse of $\mathbf{W}$) weighted by λ and added to the gradient of $\mathbf{J}_m(\mathbf{W})$. Furthermore, within the same coupled iteration loop, the rotation matrix $\mathbf{R}$ and A_{uk} are updated through the following equations:

$$\mathbf{R}_{t+1} = \mathbf{R}_t - \gamma \nabla_R(\mathbf{J}_c) \tag{9}$$

where

$$\nabla_R(\mathbf{J}_c) = 2\mathbf{R}_t\left(\mathbf{W}_{t+1}^T\mathbf{W}_{t+1}\right)^{-1} - 2\tilde{\mathbf{A}}_t\left(\mathbf{W}_{t+1}^{-1}\right)^T \quad (10)$$

is the gradient of $\mathbf{J}_c$ with respect to $\mathbf{R}$, and

$$A_{uk_{t+1}} = A_{uk_t} - \zeta\nabla_{A_{uk}}(\mathbf{J}_c) \quad (11)$$

where

$$\nabla_{A_{uk}}(\mathbf{J}_c) = 2\left(\left[A_{uk_t} - \left[\mathbf{R}_{t+1}\left(\mathbf{W}_{t+1}^{-1}\right)\right]\right.:, k+1:m\right) \quad (12)$$

is the gradient of $\mathbf{J}_c$ with respect to A_{uk}, and γ and ζ are the learning rates [Matlab notation is used to denote the last $m-k$ columns in the right-most term in (12)]. After estimating $\mathbf{W}$ in each iteration, the rotation matrix $\mathbf{R}$ and A_{uk} are also iteratively calculated in a coupled loop. Consequently, $\tilde{\mathbf{A}} = [A_k \vdots A_{uk}]$ is a good estimation of the mixing matrix and location of the sources. Sequential iteration of (7), (9), and (11) yields a robust solution to the ill-posed localization problem. Accurate selection of the learning rates μ, γ, and ζ ensures simultaneous convergence of the algorithm. The stopping condition is governed by a proper threshold on the norm of $\mathbf{W}_{t+1} - \mathbf{W}_t$. μ, γ, and ζ are initialized to $\mu_0 = \gamma_0 = \zeta_0 = 0.001$. After each iteration, they are automatically updated based on $\mu_{t+1} = \mu_0(norm(\mathbf{W}_{t+1} - \mathbf{W}_t)/norm(\mathbf{W}_t))$, $\gamma_{t+1} = \gamma_0(norm(\mathbf{R}_{t+1} - \mathbf{R}_t)/norm(\mathbf{R}_t))$, and $\zeta_{t+1} = \zeta_0(norm(\mathbf{A}\mathbf{u}_{t+1} - \mathbf{A}\mathbf{u}_t)/norm(\mathbf{A}\mathbf{u}_t))$, where $norm(.)$ denotes, for example, the Frobenius norm.

IV. Nonhomogeneity Problem

With some indeterminacy in the result, we can approximate the location of the sources within the brain. Unlike the methods in [5] and [6], which consider the sources as magnetic dipoles, we simply consider them as the sources of isotropic signal propagations. Therefore, the head (mixing medium) model only mixes and attenuates the signals. The attenuation corresponds to the distance and the resistance of the medium between the sources and the fixed electrodes. Alpha waves are recorded from the occipital and parietal regions of the cerebral cortex. However, the Alpha waves from the occipital area are prominent with higher amplitude [11], [17]. These sources generate reference signals within a small frequency band of 7–13 Hz in healthy adults, without any attention, visual, or possibly auditory stimulation and without dysfunction of the CNS. Since we can measure both the link weights and the energy of the mixtures within the selected bands, we will be able to compensate for the nonhomogenity by finding a relationship between $\tilde{\mathbf{A}}$, found through measurement of the geometrical locations, and $\mathbf{A}_g$, found through measurement of the energy of the signal(s) of the known source(s). The energy within the Alpha band is obtained by carefully bandpass filtering the EEGs around the peak in the range of Alpha frequencies. These amplitudes are then inverted to give the entries of the k columns of $\tilde{\mathbf{A}}$. On the other hand, the geometrical location of the known sources can be approximately determined offline (denoted $\tilde{\mathbf{A}}_g$). It is clear that $\tilde{\mathbf{A}} = f(\tilde{\mathbf{A}}_g)$, where f represents the nonhomogenity of the medium between the known sources and the electrodes. Instead of using the sources of normal brain rhythms as a known *a priori*, we may synthetically provide a number of sinusoidal sources in certain locations under the skull. This may be done by setting a number of electrodes under or close to the brain through the nose or mouth. No significant invasive surgical operation is needed for such purposes. In the second method, by using a set of sharp bandpass filters, projection of the sinusoidal waves to the electrodes can be easily evaluated. Therefore, the entries of $\tilde{\mathbf{A}}$ will be accurately identified. Having more known sources, the positions of the sources as well as measuring the nonlinearity resulting from the nonhomogeneity of the head, including the brain (white and gray tissues), the skull, and the scalp, can be estimated more accurately. In a spherical model of the head, we may consider three main layers: brain, skull, and scalp for which the thicknesses are known. To incorporate the nonhomogeneity, f has to be completely identified for all the sources. In some simplified practical situations, the column vectors of $\mathbf{A}$ are proportional to $1/\Gamma^2$ (rather than $1/\Gamma$).

Having more than one known source location, in order to extend the above nonlinear map to all the estimated source locations, a simple means of extrapolation of the columns of the estimated mixing matrix would be adequate.

V. Experiments

The proposed algorithm was implemented using SOBI followed by localization of the EEG sources, as described earlier. In a simulation, the mixing medium is modeled as homogenous and, in another occasion, as nonhomogenous with one and two known sources. The results were more satisfactory for two known sources for both homogenous and nonhomogenous cases. The only standing ambiguity will be the scaling problem. Although for synthetic mixtures this can be avoided by normalization, in real-life cases, additional conditions have to be involved. As stated in Section IV, the scaling factor will be equal to the ratio between the geometrical distance from the known source to the electrodes d_k and the inverse of correlation between the filtered known sources and the electrode signals C_k, i.e., d_k/C_k.

A. Using Synthetic Sinusoidal Sources

A matrix of three signals containing three synthetic sinusoidal sources with specific geometrical locations was tested. The mixing matrix $\mathbf{A}$ is modeled once with three EEG electrodes via homogenous medium and another time via nonhomogenous (only two different homogneous layers were considered, i.e., the scale factor of the mixing matrix) medium. Selection of matrix $\mathbf{A}$ was based on the true geometry of the head model and the EEG 10-20 sensor positions. The result of separation and localization were the same for both cases. The column vectors of the estimated mixing matrix A refer to the coordinates of the sources. The actual locations can be easily derived using the LS-based sphere method [16]. In Fig. 1(a), the original and simulated locations for one known source and in Fig. 1(b) with two known sources (for synthetic sources) are depicted. Using the SOBI BSS algorithm, the geometrical error $\epsilon(\epsilon = ||A_{\text{new}} - A_{\text{old}}||_2^2)$ is found to be less when the number of sources increases ($\epsilon = 0.8648$ with one known source and $\epsilon = 0.1017$ with two known sources).

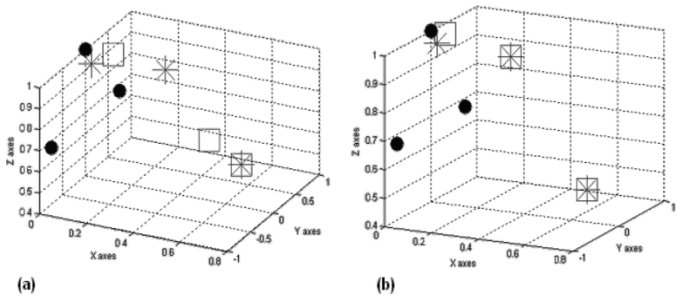

Fig. 1. Estimated source locations when (a) there is only one out of three sources known and (b) two sources are known. "•" represents the sensors locations, "∗" shows the actual locations of sources, and "□" represents the estimated locations of the sources. x, y, z are toward the front, lateral-right, and plannar views.

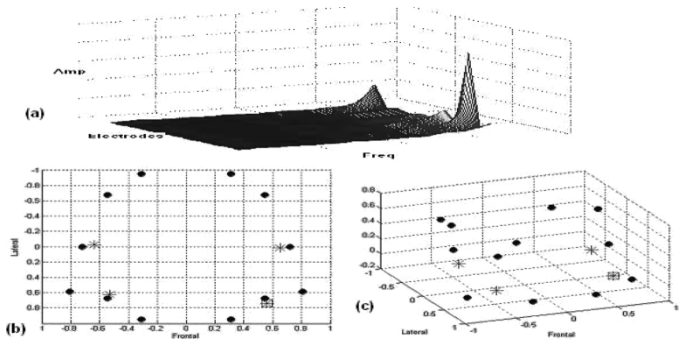

Fig. 2. Localization of the real EEG sources. (a) Selection of highest amplitude level in Alpha rhythm as for the known source explained in Section IV. (b) Top view. (c) Lateral perspective view of the locations of electrodes shown by "•," the location of the known source shown by "□," and the estimated locations of the unknown sources shown by "∗."

B. Using Real EEG Signals

For localization, the signals include the EEGs for focal epilepsy with confirmed epileptic foci and normal EEG with both Delta and Alpha rhythms (considering Alpha rhythm to be the known and Delta rhythm to be the unknown sources). The electrodes were set up according to [19]. The location of the known source is shown in Fig. 2(a). After the artifact removal technique used in [18], the estimated location of unknown sources can be observed in Fig. 2(b) and (c) for clarity. In Fig. 2(b), it is obvious that the epileptic foci are located around the fronto-temporal regions of the brain.

VI. Conclusion

In this letter, *a priori* knowledge about the known EEG sources and their locations have been effectively exploited in localization of the other sources separated based on a partially constrained BSS method. Unlike dipole-based methods, the proposed algorithm is computationally cost effective and is insensitive to noise (noise is either separated or cancelled out due to the inherent properties of the BSS). The normal brain rhythms with given sources locations can be considered as the known sources. The known sources may also be generated synthetically. The existence of a normal brain rhythm can be checked by examining the spectrum of the signals in various conventional frequency bands. In the algorithm, the unknown sources as well as the permutation matrix and the unmixing matrix are determined. The columns of the estimated $\mathbf{A}$, then, refer to the locations of the sources. The LS-based sphere method is finally used to obtain the estimated geometrical locations. The accuracy of the results increases with the increase in the number of known sources.

References

[1] R. O. Schmidt, "Multiple emitter location and signal parameter estimation," in *Proc. RADC Spectrum Estimation Workshop*, New York, 1979, pp. 243–258.

[2] D. Gutiérrez and A. Nehorai, "Estimating brain conductivities and dipole source signals with EEG arrays," *IEEE Trans. Biomed. Eng.*, vol. 51, no. 12, pp. 2113–2122, Dec. 2004.

[3] C. H. Muravchik and A. Nehorai, "EEG/MEG error bounds for a static dipole source with a realistic head model," *IEEE Trans. Signal Process.*, vol. 49, no. 3, pp. 470–484, Mar. 2001.

[4] M. Scherg and D. Von Cramon, "Two bilateral sources of the late AEP as identified by a spatio-temporal dipole model," *Electroenceph. Clin. Neurophysiol.*, vol. 62, pp. 290–299, 1985.

[5] J. C. Mosher and R. M. Leahy, "Source localization using recursively applied and projected (RAP) MUSIC," *IEEE Trans. Signal Process.*, vol. 47, no. 2, pp. 332–340, Feb. 1999.

[6] R. M. Leahy, "A study of dipole localization accuracy for MEG and EEG using a human skull phantom," *Electroenceph. Clin. Neurophysiol.*, vol. 107, pp. 159–173, 1998.

[7] R. D. Pascual-Marqui, C. M. Michel, and D. Lehmann, "Low resolution electromagnetic tomography: A new method for localizing electrical activity in the brain," *Int. J. Psychophysiol.*, vol. 18, pp. 49–65, 1995.

[8] J. Muscat, R. Grech, K. P. Camilleri, S. G. Fabri, and C. J. James, "An improvement in EEG forward model computational efficiency," in *Proc. 2nd Int. Conf. Advanced Biomedical Signal Information Processing*, 2004, pp. 99–103.

[9] W. Wang, J. A. Chambers, and S. Sanei, "A joint diagonalization method for convolutive blind separation of nonstatioanry sources in the frequency domain," in *Proc. ICA*, Nara, Japan, 2003, pp. 939–944.

[10] A. J. van der Veen, "Joint diagonalization via subspace fitting techniques," in *Proc. IEEE ICASSP* , Salt Lake City, UT, 2001.

[11] California University.. [Online]http://www.csun.edu/vcpsy00i/dissfa01/EEG lesson.html

[12] C. Phillips, M. D. Rugg, and K. J. Friston, "Anatomically informed basis functions for EEG sources localization: Combining function and anatomical constraints," *NeuroImage*, vol. 16, pp. 678–695, 2002.

[13] R. D. Pascaul-Marqui, M. Esslen, K. Kochi, and D. Lehmann, "Functional imaging with low resolution brain eletromagnetic tomography (LORETA): A review," *Methods Findings Exper. Clin. Pharmacol.*, vol. 24C, pp. 91–95, 2002.

[14] J. Yao and J. P. A. Dewald, "Evaluation of different cortical source localization methods using simulated and experimental EEG data," *NeuroImage*, vol. 25, pp. 369–382, 2005.

[15] E. Niedermeyer, "Alpha rhythm as physiological and abnormal phenomena," *Int. J. Psychophysiol.*, vol. 26, no. 1–3, pp. 31–49, Jun. 1997.

[16] I. D. Coope, "Reliable computation of the points of intersection of n spheres in $\mathbb{R}^n$," *ANZIAM J.*, vol. 42, no. E, pp. C461–C477, 2000.

[17] P. J. Marshall, Y. Bar-Haim, and N. A. Fox, "Development of the EEG from 5 months to 4 years of age," *Clin. Neurophysiol*, vol. 113, pp. 1199–1208, 2002.

[18] L. Shoker, S. Sanei, and M. A. Latif, "A new constrained BSS algorithm for separation of EEG signals with eye-blinking artifact," in *Proc. 3rd IEEE Sensor Array Multichannel Signal Processing Workshop*, Barcelona, Spain, 2004.

[19] J. H. Margerison, C. D. Binnie, and I. R. McCaul, "Electroencephalographic signs employed in the location of ruptured intracranial arterial aneurysms," *Electroencephalogr. Clin. Neurophsiol.*, pp. 296–306, Jul. 1969.

[20] A. C. Tang, M. T. Sutherland, and C. J. McKinney, "Validation of SOBI components from high-density EEG," *NeuroImage*, vol. 25, pp. 539–553, 2004.

[21] C. Philips, M. D. Rugg, and K. J. Friston, "Systematic regularization of linear inverse solutions of the EEG source localization problem," *NeuroImage*, vol. 17, pp. 287–301, 2002.